Tapered Partially Reflective Surface Amplitude Distribution for High Gain and Low Side Lobe Level

Muhammad Hussain, Dongho Kim, Kyung-Geun Lee*
Sejong University
engrhussain2010@sju.ac.kr, dongkim@sejong.ac.kr, kglee@sejong.ac.kr

요 약

The Fabry-Perot cavity antenna (FPCA) has been extensively explored in the literature for the accelerated advancement of the 5G next-generation networks due to its conceivable attributes (high gain, significance bandwidth, and low sidelobe level (SLL)). However, high sidelobes make it difficult to achieve maximum radiation efficiency. In this article, tapered partially reflective surface (PRS) reflection amplitude distribution has been proposed to improve high gain with suppressed SLL. The novel tapered distribution is intended with manipulated phase consideration of the FPCA to achieve a high realized gain 17.2 dBi with suppressed SLL −20.3 dB and −16.5 dB in E- and H-planes, respectively. We confirm that the proposed scheme can achieve a good radiation pattern in the broadside direction by CST studio suite simulations.

I. Introduction

The FPC has accomplished plausible significance in the wireless communication industry due to its innovative outcomes. An appropriate counterpart of the FPC is high gain with low-profile fabrication in next-generation mobile communications. However, relatively high sidelobes are an obstacle to provide optimum radiation efficiency. This issue opens a new window for researchers to enhance the radiation efficiency of FPC antennas (FPCAs).

In prior publications, the plethora of scientific mechanism has been proposed to investigate the antennas, which includes a transmission line (TL) [1], and ray theory (RT) [2]. RT is the good approach to analyze an FPCA. Therefore, research candidates use the RT method to obtain the high realized gain, significant bandwidth, and low SLL [3]. Recently, in [4], Hayat et al. have introduced a phase rectifying transparent superstrate (PRTS) — polylactic acid (PLA): t = 21mm — over a PRS surface to obtain a nearly planar wavefront. However, overall FPC size have been increased which is not suitable for low-profile fabrication design. In [5], a permittivity gradient superstrate (PGS) — acrylo-butadiene styrene (abs): $\varepsilon = 2.1 \rightarrow 2.8$, t = 13.5mm — has been proposed as a PRS without any inductive and capacitive layers. The phase delay was produced to obtain a planar wavefront by introducing the PGS. Fabrication of a single superstrate with multiple permittivity properties is challenging which designed with a 3D printer [5]. However, permittivity gradient superstrate (PGS) is not commercially available.

In this work, we present a transverse electric (TE) hybrid mode with tapered PRS magnitude distribution of an FPC antenna at 5 GHz, capable of achieving high realized gain, low sidelobe level in E/H planes, simultaneously.

II. FPC Antenna Design

The 2D ray tracing model depicted in Fig. 1, in which a PRS and an artificial magnetic conductor (AMC) are designed to ensure constructive interference (CI) within the FPC. With respect to ray theory, phase delays of all rays (E_1 to E_n) have been calculated at the wave-front to satisfy the Trentini's beam forming condition (1) [2] in the broadside direction. S the center of a stacked aperture-coupled MSA, a feeding source operating at f_o = 5 GHz. The polarization of the source is along the x-axis. N is the total number of unit cells on the PRS and the AMC, from the center to the end of the FPC.

$$\phi_{\Gamma n}^{\mathrm{PRS}} - 2\beta h_c^{FPC} - \pi = \pm 2N\pi \qquad (1)$$

Here, h_c is the FPC height to satisfy the resonance condition with a slanted incident angle α at the center position of every PRS unit cell. The reflection magnitude tapering has been defined along the y-axis for the TE mode, which follows (2) [6].

$$A_n = A\left(1-\frac{2}{l}\left|y'_N\right|\right) \qquad (2)$$

where, A is the reflection amplitude of the PRS unit cell and l is the length of the FPC antenna physical aperture that is $4.3\lambda_o \times$

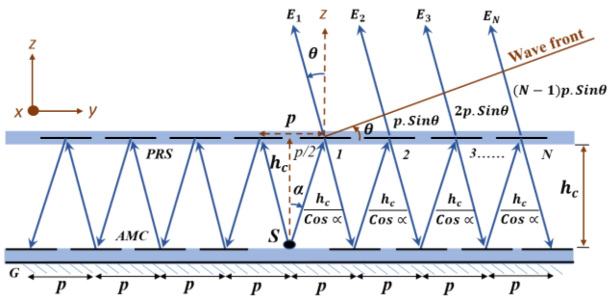

Figure 1. 2D ray tracing model for FPC antenna

$4.3\lambda_o$. y' is the distance between the center of the PRS unit cell and the middle position ($2.15\lambda_o$) of the PRS superstrate. The phase responses of the PRS unit cells will not be manipulated due to the selection of the tapered reflection amplitude distribution. Therefore, FPC's phase response has been manipulated with the reflection phases of the AMC unit cells to satisfy Trentini's condition [2]. Hence, constructive interference has been ensured within the FPC. Tapered reflection amplitude distribution has been proposed over the PRS for a TE hybrid mode. The tapered reflection amplitude distribution's results will be compared to the traditional uniform reflection amplitude distribution's results. In the traditional uniform distribution, uniform reflection amplitude distribution of the PRS unit cells is defined. In the tapered TE hybrid mode, however, tapering reflection amplitude distribution of the PRS unit cells is defined for a TE mode (along the y-axis) incidence. Only one middle row of AMC unit cells is designed for a TM mode incidence (along the x-axis).

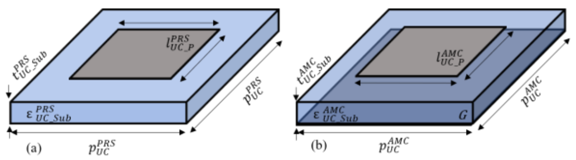

Figure 2. Unit cells (a). PRS Unit Cell, (b). AMC Unit Cell

The schematic of the PRS and AMC unit cells are shown in Fig. 2(a) and Fig. 2(b), respectively. The reflection and transmission characteristics of these unit cells have been

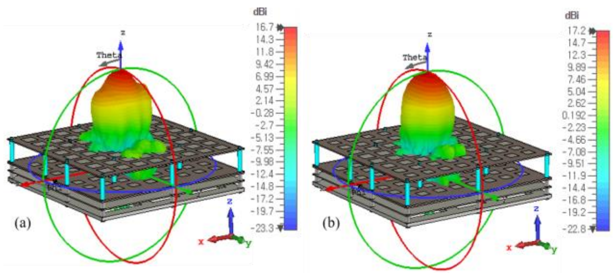

Figure 3. 3D Radiation Pattern of the (a). Uniform TE Mode, (b). Tapered TE Hybrid Mode

optimized using five parameters; periodicity *p*, length *l*, incident angle *α*, thickness *t*, and permittivity *ε* of the Taconic (RF-35: ε = 3.5, δ = 0.0025) substrate.

III. FPC Antenna Simulated Results

Figure 3 illustrates the 3D radiation pattern of the FPCA's realized gain. The simulated results of the FPCA are taken by CST studio suite. The maximum realized gain attains 16.7 dBi and 17.2 dBi for the uniform and the tapered cases at 5 GHz, respectively.

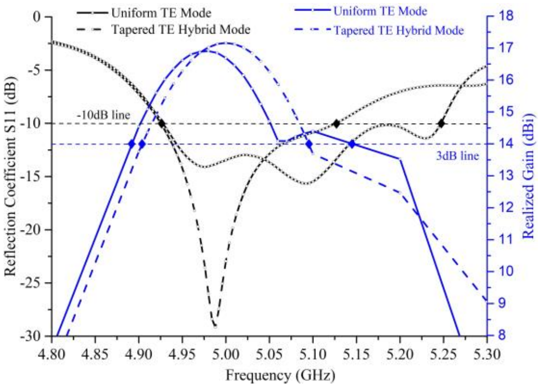

Figure 4. Reflection coefficient S_{11} and 3 dB gain bandwidth of the uniform TE mode and tapered TE hybrid mode of FPCA.

Figure 4 depicts a reflection coefficient S_{11}, and a 3 dB gain bandwidth of the FPCA. The Bandwidth efficiency has been assessed for the uniform and the tapered cases, which is 79 % and 92 %, respectively.

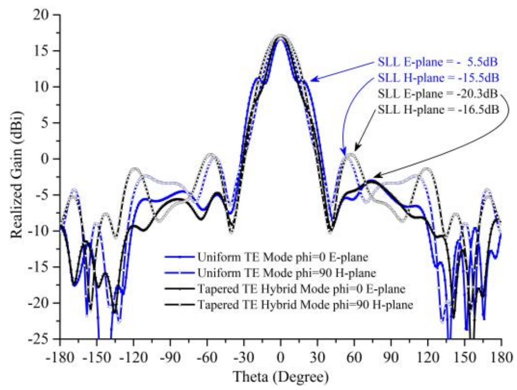

Figure 5. 2D radiation pattern of the uniform TE mode and tapered TE hybrid mode of FPCA in E-plane phi = 0° and H-plane phi = 90°.

Similarly, SLL suppression has been depicted in Fig. 5. Here, the proposed FPCA model for the tapered TE hybrid mode has attained a SLL = −20.3 dB in an E-plane and a SLL = −16.5 dB in an H-plane. All other properties for scrutinizing the FPCA are compared in Table 1.

Table 1. Properties comparison of uniform TE mode and tapered TE hybrid mode

Properties	Uniform TE Mode	Tapered TE Hybrid Mode
Radiation Efficiency	89 %	90 %
Total Efficiency	85 %	90 %
Aperture Efficiency	20 %	22.5 %
Bandwidth (-10dB)	319 MHz	201 MHz
Realized Gain	16.7 dBi	17.2 dBi
3dB Gain Bandwidth	253 MHz	191 MHz
Bandwidth Efficiency	79 %	95 %
SLL E-plane phi=0°	−5.5 dB	−20.3 dB
SLL H-plane phi=90°	−15.5 dB	−16.5 dB

To emphasize the efficacy of our work, Table 2 compares the radiation performance of the proposed PRS with some of recently published superstrates. The FPCA has comparable performance with its counterparts in terms of realized gain, PRS thickness, and SLL.

Table 2. Comparison of PRS with other superstrates

Ref.	PRS	PRS thickness	Realized Gain	SLL (E-plane)	SLL (H-plane)
[4]	Double layer	30.1 mm	18 dBi	−18 dB	−17 dB
[5]	Single layer	13.5 mm	14 dBi	−10.4 dB	−12.7 dB
Ours	Single layer	1.52 mm	17.2 dBi	−20.3 dB	−16.5 dB

IV. Conclusion

In this research work, we investigated the tapered reflection amplitude distribution of the PRS to attain the maximum realized gain with minimum SLL. Using this topology, proposed FPCA achieves 95 % bandwidth efficiency, 17.2 dBi realized gain with minimum SLL −20.3 dB and −16.5 dB in E-plane and H-plane, respectively. The proposed FPCA is 90 % efficient overall. Therefore, our antenna will play a key role in ensuring the reliability of wireless communication networks.

Acknowledgment

This research work was supported by Basic Science Research Program of the National Research Foundation (NRF) of Korean Government (MSIT) under Grant 2018R1D1A1A09082807 and 2020R1A2C2013466.

References

[1] F. Costa, D. Bianchi, A. Monorchio, and G. Manara, "Linear Fabry-Perot/leaky-wave antennas excited by multiple sources," IEEE Transactions on Antennas and Propagation, vol. 66, no. 10, pp. 5150-5159, 2018.

[2] G. V. Trentini, "Partially reflecting sheet arrays," IRE Transactions on antennas and propagation, vol. 4, no. 4, pp. 666-671, 1956.

[3] A. Goudarzi, M. M. Honari, and R. Mirzavand, "Resonant Cavity Antennas for 5G Communication Systems: A Review," Electronics, vol. 9, no. 7, p. 1080, 2020.

[4] T. Hayat, M. U. Afzal, A. Lalbakhsh, and K. P. Esselle, "3-D-printed phase-rectifying transparent superstrate for resonant-cavity antenna," IEEE Antennas and Wireless Propagation Letters, vol. 18, no. 7, pp. 1400-1404, 2019.

[5] T. Hayat, M. U. Afzal, F. Ahmed, S. Zhang, K. P. Esselle, and J. Y. C. Vardaxoglou, "Low-Cost Ultra-Wideband High-Gain Compact Resonant Cavity Antenna," IEEE Antennas and Wireless Propagation Letters, 2020.

[6] C. A. Balanis, "Antenna theory analysis and design, A JOHN WILEY & SONS," Inc., Publication, 2005.